Increased Apoptosis Arising from Increased Expression of the Alzheimer's Disease–associated Presenilin-2 Mutation (N141I)

Susan Janicki and Mervyn J. Monteiro

Medical Biotechnology Center of the University of Maryland Biotechnology Institute and Departments of Molecular Biology and Biophysics, Neurology, and Human Genetics, Baltimore, Maryland 21201

Abstract. Mutations in the genes for presenilin 1 and 2 (PS-1 and PS-2) have been linked to development of early-onset Alzheimer's disease (AD). As neither the normal function of either presenilin is known nor why mutations cause disease, we examined the properties of wild-type, truncated, and mutant PS-2 upon expression in HeLa cells. Although HeLa cells are strongly predisposed to continued mitosis, expression of PS-2 induced programmed cell death (apoptosis). Direct evidence for apoptosis was obtained by double staining for terminal deoxynucleotide transferase nick end labeling (TUNEL) and PS-2 expression and by following green fluorescent protein–tagged PS-2 over time. Deletion analysis indicates that as little as 166 NH_2-terminal residues of PS-2 are sufficient for endoplasmic reticulum (ER) localization and apoptosis. Moreover, the AD-associated PS-2 missense mutation (N141I) more efficiently induced cell death compared to wild-type PS-2 despite lower mutant protein accumulation. Expression of the presenilins in several other cell lines and transgenic mice has been accompanied by rapid protein cleavage without the induction of cell death. In contrast, PS-2 expressed in HeLa cells was not cleaved, and cell death occurred. We hypothesize that full-length but not cleaved PS-2 may be important in the regulation or induction of apoptosis.

Alzheimer's disease (AD)[1] is a neurodegenerative disorder manifesting with increasing incidence in the aging population. Clinically, it is characterized by memory loss and declining cognitive functions. Familial studies, especially in early-onset cases, indicate molecular heterogeneity and have linked AD to mutations in at least three genes: the β-amyloid precursor protein gene (βAPP) located on chromosome 21 (for review see Mullan and Crawford, 1993) and the presenilin 1 and 2 (PS-1 and PS-2, respectively) genes located on chromosome 14 and 1, respectively (Alzheimer's Disease Collaborative Group, 1995; Campion et al., 1995; Chapman et al., 1995; Cruts et al., 1995; Levy-Lahad et al., 1995*a*,*b*; Perez-Tur et al., 1995; Rogaev et al., 1995; Sherrington et al., 1995; Wasco et al., 1995; Boteva et al., 1996). In addition, there is evidence that the acquisition of the apolipoprotein E type 4 (APOE-E4) allele on chromosome 19 predisposes individuals to early onset of AD (Corder et al., 1993; Strittmatter and Roses, 1995).

Address all correspondence to Mervyn J. Monteiro, Ph.D., University of Maryland Biotechnology Institute, Room N352, 725 West Lombard Street, Baltimore, MD 21201. Tel.: (410) 706-8132. Fax: (410) 706-1732.

1. *Abbreviations used in this paper*: aa, amino acid(s); AD, Alzheimer's disease; βAPP, β-amyloid precursor protein gene; CMV, cytomegalovirus; DAPI, 4′6-diamidino-2-phenylindole; GST, glutathione-S-transferase; PS-1 and -2, presenilin 1 and 2; TMD, transmembrane domain.

Mutations in βAPP account for ~5% of familial cases (~19 families) with six different single or double missense mutations described so far (for review see Haass et al., 1995; Van Broeckhoven, 1995). The larger proportion of familial AD patients (50–70% of all cases >50 families) have mutations within the PS-1 gene, which has been shown to be a hot spot for missense mutations, as greater than 35 different mutations have been identified so far (for review see Cruts et al., 1996; Haass, 1997). Interestingly, the age of onset of AD correlates somewhat with the location of mutations within the coding regions of PS-1 (for review see Cruts et al., 1996). Fewer AD cases are associated with mutations in PS-2 as only two missense mutations have been described in eight families, mainly of Volga-German descent (Levy-Lahad et al., 1995*a*,*b*; Rogaev et al., 1995), and recent evidence indicates at least one of these mutations is variably penetrant (Sherrington et al., 1996).

PS-1 and PS-2 are highly homologous by sequence comparison with the highest degrees of variability occurring in the amino- and carboxyl-terminal regions. Although the function of these proteins is not known, they share homology with two *Caenorhabditis elegans* proteins. The presenilins are ~50% homologous to Sel-12, which is involved in cell signaling by Notch-based receptors, and they exhibit limited homology to SPE-4, which functions in spermatogenesis (Levitan and Greenwald, 1995; Levy-Lahad et al., 1995; Sherrington et al., 1995). Evidence suggesting

that these putative *C. elegans* homologues may indeed be related to mammalian presenilins is the apparent ability of injected human PS-1 and PS-2 cDNAs to functionally rescue a *C. elegans* Sel-12 mutant defective in vulva development and egg laying (Levitan et al., 1996). Additional evidence indicating PS involvement in development are recent reports showing molecular disruption of the PS-1 gene leads to death shortly after birth with embryos displaying central nervous system defects together with abnormal patterning of the axial skeleton and spinal ganglia (Shen et al., 1997; Wong et al., 1997).

Both presenilin genes are ubiquitously expressed with differential accumulation of two major mRNA transcripts (Li et al., 1995; Rogaev et al., 1995; Sherrington et al., 1995; Lee et al., 1996; Vito et al., 1996*a*,*b*). Immunofluorescence staining of epitope-tagged presenilins indicates that the proteins are localized to the ER and Golgi, although subtle differences in localization between PS-1 and PS-2 were noted (Cook et al., 1996; Kovacs et al., 1996; Walter et al., 1996). The presenilins are multipass transmembrane proteins that are believed to topologically weave through ER membranes six to eight times with the NH_2- and COOH-terminal domains and the large "loop" spanning the putative sixth and seventh transmembrane domains (TMDs) (according to some models) contained within the cytoplasm (see Fig. 1; Doan et al., 1996; Li and Greenwald, 1996; Lehmann et al., 1997). Recent studies of PS-1 expression in fibroblasts and transgenic mice indicate that PS-1 is proteolytically cleaved since 27–28-kD NH_2-terminal and 16–17-kD COOH-terminal derivatives accumulate in cell lysates (Lee et al., 1996; Thinakaran et al., 1996). Analogous proteolytic cleavage of PS-2 has also been reported (Kim et al., 1997; Tomita et al., 1997). The function of proteolytic cleavage of the presenilins is not known.

To study the function of presenilins, we cloned and expressed wild-type, mutant, and deleted forms of human PS-2 in HeLa cells, a human cell line typically resistant to apoptosis. Our studies show that the overexpression of PS-2 in HeLa cells affects nuclear morphology and causes cell death. Furthermore, we demonstrate that 166 NH_2-terminal PS-2 residues are sufficient for ER localization and for inducing cell death. Most interestingly, we demonstrate the AD-associated PS-2(N141I) mutation induces an increase in cell death of HeLa cells compared to wild-type PS-2.

Materials and Methods

Cloning of Human PS-2 cDNA and Construction of PS-2 Variants

The PS-2 cDNA was obtained from a human brain marathon-ready cDNA library (CLONTECH Laboratories, Inc., Palo Alto, CA) by PCR amplification using two primers, a 5′-end primer (5′ATCGATAAGCTTCGCGAGTGTTCGTGGTGCTTCCAGAGGCA3′) of which 25 bases of the 3′ end of the primer were identical to the coding strand of human PS-2 six bases upstream of the ATG start codon, and a 3′-end primer (5′GGAAGAATTCGTCGACGCAGCCTGTGGCACACCATGTCCC3′) of which 24 bases of the 3′ end were complementary to sequences immediately downstream of the PS-2 stop codon. The PCR reaction was carried out according to instructions provided by the manufacturer. A major PCR product of ~1.4-kbp spanning the entire coding sequence of PS-2 was produced. The PCR product was digested with EcoRI since this site was engineered into the 3′-end primer and the resulting ~1.4-kbp product was ligated into plasmid pBluescript KS(−) that had been previously digested with EcoRV and EcoRI. The recombinant plasmid was fully sequenced and was found to correspond to human PS-2 without any of the known AD mutations (Levy-Lahad et al., 1995*a*; Rogaev et al., 1995).

To express PS-2 in human cells, full-length PS-2 and four progressively shorter COOH-terminal deletions were cloned into a pGEM expression vector such that the PS-2 cDNA was placed in the appropriate orientation for expression from the strong cytomegalovirus (CMV) promoter (Fig. 1). The pGEM CMV-driven expression plasmid was constructed from pCMV-NF-L (Lee et al., 1993; was kindly provided by Dr. Michael Lee, Johns Hopkins University, Baltimore, MD) by first destroying the most 5′ EcoRI site in the vector by standard molecular techniques. The product was then double digested with EagI, which cleaves just 3′ of the CMV promoter in NF-L 5′ untranslated sequences (see Monteiro et al., 1994), and HindIII, which is located at the 3′ end of the NF-L fragment (Lee et al., 1993). Next, through a series of cloning steps an EagI-HindIII fragment from pNF(+La/head) containing lamin 5′ sequences, 12 codons of myc sequence, and the entire NF-L 3′ region (Monteiro et al., 1994) was introduced into the CMV expression vector. This plasmid was then double digested with SacII, which is located 3′ of the EagI site in the 5′ untranslated sequence of lamin A, together with SalI, which cleaves 5′ of the myc sequences. PS-2 fragments digested with SacII and SalI were subsequently ligated into this CMV expression vector.

pPS-2+MYC

To express full-length PS-2 tagged with the myc epitope, the PS-2 cDNA was PCR amplified with primers that introduced a SacII site upstream of the ATG and a SalI site at the 3′ end, which eliminated the stop codon and fused the protein to the myc sequence (described in Monteiro et al., 1994). The 5′-end primer, 5′ACGTACGTAACCGCGGGTTCGTGGTGCTTCCAG3′, contained a SacII site followed by 17 bases at its 3′ end, which were identical in sequence to the coding strand of PS-2 with similarity beginning 10 bp upstream of the ATG start codon. The 3′-end PCR primer, 5′TATCGCTTAAGTCGACGATGTAGAGCTGATGGG3′, contained 17 bases complementary to sequences just upstream of the stop codon of PS-2 and was preceded by a SalI restriction site. The ~1.4-kbp PCR product was double digested with SacII and SalI and ligated into the pGEM CMV vector (Fig. 1 *C*).

pPS-2

To express full-length PS-2 (encoding 448 amino acids [aa]; Fig. 1 *A*) that was not myc tagged, PS-2 cloned in Bluescript and pPS-2+Myc were each double digested with NotI and EcoRI. NotI cuts at codon 111 of PS-2, whereas the EcoRI site was located downstream of the stop codon in both plasmids. The 3′-end fragment of PS-2 that was devoid of myc sequences and derived from the Bluescript vector was used to replace the corresponding myc-tagged fragment in the pPS-2+Myc.

Construction of pPS-2(268aa)+Myc, pPS-2(222aa)+Myc, and pPS-2(166aa)+Myc Constructs

To create PS-2 constructs with progressively longer COOH-terminal deletions, the previously described 5′ primer containing the SacII site was used in conjunction with 3′ primers designed to introduce SalI sites into the PS-2 gene, which allowed the truncated proteins to be myc tagged.

pPS-2(268aa)+Myc. A 3′ primer, 5′TATCGCTTAAGTCGACCAGCACAGCCACGAGAT3′, containing 17 bases homologous and complementary to sequences upstream of codon 268 was used to generate construct pPS-2(268aa)+Myc using essentially the same procedure previously described for the construction of pPS-2-Myc. This construct is deleted of 180 COOH-terminal residues immediately 3′ of the sixth putative TMD, thereby removing the large hydrophilic loop and all COOH-terminal sequences (Fig. 1 *D*).

pPS-2(222aa)+Myc. By a similar PCR procedure, 226 residues from the COOH terminus of PS-2 were deleted using a 3′ primer, 5′TATCGCTTAAGTCGACCTTCCAGTGGATGCACA3′, which contained 17 bases homologous and complementary to sequences upstream of codon 222. The resulting construct pPS-2(222aa)+Myc is therefore deleted of PS-2 sequences beginning three residues downstream of TMD 4 (Fig. 1 *E*).

pPS-2(166aa)+Myc. Similarly, the primer 5′TATCGCTTAAGTCGACCTTGATGCAGCGGTACT3′, of which the last 17 bases were homologous and complementary to sequences upstream of codon 166 of PS-2, deleted 282 aa beginning six residues downstream of TMD2 (Fig. 1 *F*).

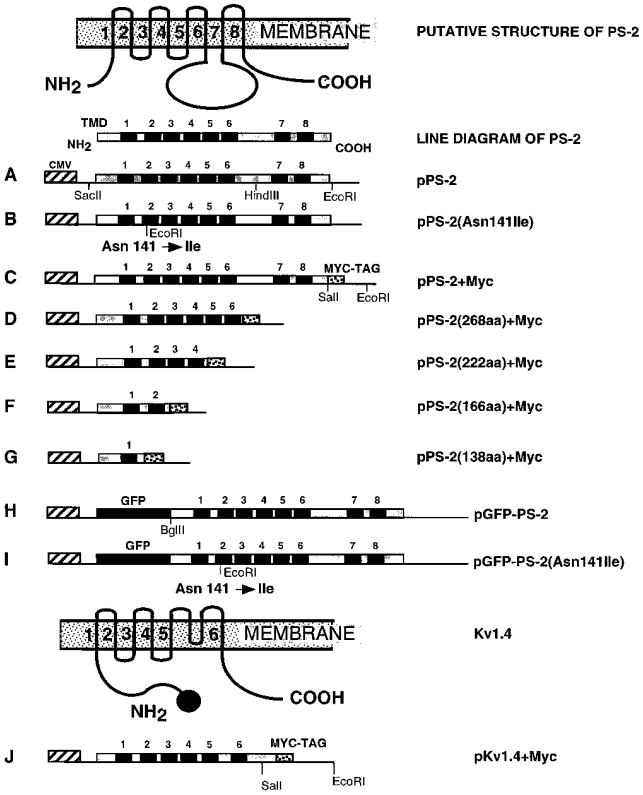

Figure 1. Schematic drawings of PS-2 expression constructs. The putative structure of PS-2 is shown. The schematic with a corresponding line drawing illustrates PS-2 with eight TMDs (numbered 1–8). NH_2-, COOH-terminal, and the large hydrophilic loop domains are all present on the cytoplasmic side of an ER membrane. (*A–I*) PS-2 expression constructs used in this study. Some of the restriction sites used for cloning are shown. Transcription of all constructs was driven by the CMV promoter. The constructs that were myc- or GFP-tagged are illustrated. Constructs *B* and *I* contain the AD-associated PS-2(N141I) mutation. Construct *J* is a line drawing of the Kv1.4 human potassium channel cDNA that was used as a control since it is similar in topology (shown schematically) to PS-2.

pPS-2(138aa)+Myc. Primer 5′ACGTACGTAAGTCGACGGAGTTGAGGAGGCGCT3′, of which the last 17 bases were homologous and complementary to sequences upstream of codon 138 of PS-2, was similarly used to delete 310 COOH-terminal residues of PS-2, including TMD2 (Fig. 1 *G*).

pGFP-PS-2 and pGFP–PS-2(Asn141Ile)

To monitor PS-2 expression in living cells, PS-2 was cloned into the CLONTECH pEGFP-C1 expression vector, thus fusing PS-2 to the COOH-terminal end of *Aequorea victoria* GFP. To generate this clone, a 5′ primer, 5′TCCGGACTCAGATCTCTCACATTCATGGCCTCT3′, of which the last 18 bp were identical to sequences starting at codon 2 of PS-2, was used in combination with the 3′ primer, 5′TATCGCTTAAGTCGACGATGTAGAGCTGATGGG3′ (described above), to PCR amplify PS-2 clone in Bluescript. The ~1.4-kbp product was digested with BglII, which was introduced by the 5′-end primer, and HindIII, which cuts PS-2 internally. The ~1-kbp fragment was then ligated between the BglII-HindIII sites of pEGFP-C1. The recombinant pGFP–PS-2(Δ86) missing 86 COOH-terminal residues of PS-2 was then digested with HindIII and EcoRI, the latter cutting 3′ of the former. In conjunction, PS-2 in Bluescript was digested with the same enzymes, and the fragment containing the 3′ coding sequences of PS-2 was ligated with the pGFP–PS-2(Δ86) plasmid fragment. The resulting recombinant yielded pGFP–PS-2 corresponding to full-length PS-2 (missing only the start methionine residue) fused in frame COOH-terminal of GFP (Fig. 1 *H*).

An additional GFP–PS-2 fusion construct was made to express the PS-2(Asn141Ile) AD-associated mutation (Levy-Lahad et al., 1995*a*; Rogaev et al., 1995). The asparagine codon at position 141 in PS-2 was converted to an isoleucine by a two-step PCR amplification protocol. In the first step, the 5′ portion of PS-2 was amplified using the 5′ BglII-containing primer described above in conjunction with a 3′ primer, 5′CGTAACGCGAATTCAGGAGGCGCTGGCCCACC3′. The remaining PS-2 3′ segment was amplified with a 5′ primer, 5′TCAAGCTTGAATTCCGTGCTGATCACCCTCATCATGATCA3′, and the PS-2 3′-end primer described initially. Both PCR products were cut with EcoRI, which was introduced by the new primers, and the segments linked in frame with GFP to yield pGFP–PS-2(N141I) (Fig. 1 *I*). This and the other clones that were generated by PCR were sequenced and were found to encode the expected changes.

pPS-2–(N141I)

To express full-length PS-2 containing the AD-associated mutation, PS-2(N141I), which was neither tagged with GFP nor myc sequences (Fig. 1 *B*), the XmaI-HindIII fragment from pPS-2 spanning the Asn codon at 141 of wild-type PS-2 was replaced with the corresponding fragment containing the mutation from pGFP–PS-2(N141I) to yield pPS-2(N141I) (Fig. 1 *B*).

pKv1.4+Myc

A human fetal brain cDNA library (CLONTECH Laboratories, Inc.) was screened by DNA hybridization with a 1.5-kbp EcoRV-EcoRI subfragment of human heart potassium channel Kv1.4 cDNA (kindly provided by Dr. M. Tamkun, Vanderbilt University, Nashville, TN). One positive clone, containing a 3,023-bp cDNA, was fully sequenced and had an open reading frame of 653 amino acids that was homologous to potassium channel Kv1.4 (Tamkun et al., 1991). Through a series of cloning steps, the cDNA was inserted into the modified CMV expression construct, described above, such that the cDNA was fused in-frame at codon 653 of its open reading frame with the myc tag for expression. Transfection of this construct into HeLa cells and electrophysiological recordings using the whole cell patch clamp technique revealed classical voltage-gated activation and inactivation kinetics of an A-type potassium channel.

Expression of Glutathione-S-Transferase (GST)–PS-2 Fusion Proteins in Bacteria

Three different portions of PS-2, the NH_2-terminal, the loop spanning TMD 6 and 7, and the COOH-terminal regions (see Fig. 1), were expressed as GST fusion proteins in bacteria. To express the PS-2 NH_2-terminal sequences, the segment encoding the first 86 residues of PS-2 were PCR amplified with a 5′ primer, CGTACGTCGAATTCCCAATGCTCACATTCATGGC, which introduced an EcoRI site and a proline codon one amino acid upstream of the PS-2 start codon, and a 33 bp 3′ primer, GCTGAGTACGCTCGAGCTTCGCTCCGTATTTGA, which introduced a XhoI site after residue 86. Similarly, the segment encoding 120 amino acids of the loop sequence, from residue 270 to residue 389, were PCR amplified with a 5′ primer, CGCTTCTGGAATTCCCCAAAGGGCCTCTGAG, which introduced an EcoRI site before residue 270, and a 3′ primer, GCTGAGTACGCTCGAGCAGCGTGGTATTCCAGT, which introduced an XhoI site after residue 389.

The COOH-terminal segment encoding the last 39 PS-2 residues was amplified with a 28-bp 5′ primer, CGGTACGTGAATTCAAGAAGGCGCTGCC, which introduced an EcoRI site before residue 410 and the previously described 3′ primer used to introduce a SalI site into the end of full-length PS2 to myc tag it.

The ~260-bp NH_2-terminal and 360-bp loop PCR products and the Pharmacia pGST/His T1 vector (Pharmacia Biotech, Inc., Piscataway, NJ) were all digested with EcoRI and XhoI. The ~120-bp COOH-terminal PCR fragment was cut with EcoRI and SalI. The fragments were all ligated into pGST/His T1 with the COOH-terminal insertion destroying the XhoI site. These ligations resulted in the fusion of PS-2 sequences COOH-terminal and in-frame with GST. The resulting recombinant plasmids were transformed into CAG456 bacteria (Mercy et al., 1992) and grown overnight at 30°C in 30 ml of standard Luria Broth containing 50 μg ampicillin per ml. The cultures were then diluted into 500 ml of fresh medium and grown for a further 2 h. IPTG was then added to 0.1 mM, and the cultures grown for 3–4 h. The bacteria were collected by centrifugation for 30 min at 3,000 *g*

and resuspended in 1/10 vol chilled 50 mM Tris, pH 7.5, 10% sucrose solution. The following steps were all done on ice: Lysozyme was added to 0.2 mg/ml and left for 20 min with occasional mixing followed by EDTA to 5 mM, NP-40 to 0.1%, and sarkosyl to 0.25%. After a 10-min incubation on ice, the lysed bacteria were sonicated and spun at 4°C for 30 min at 30,000 *g*. The pellet was removed and the soluble bacterial proteins were incubated for 17 h on a rocker with swollen and equilibrated glutathione agarose beads (Sigma Chemical Co., St. Louis, MO). The slurry was centrifuged at 3,000 *g* for 5 min, the supernatant was removed, and the agarose pellet was washed in chilled PBS five or six times. GST fusion proteins were eluted in batch with four consecutive bed volume elutions of 10 mM reduced glutathione in 50 mM Tris, pH 8. The eluted fractions were dialyzed in 50 mM Tris, pH 7.5, 10% sucrose, and 5 mM EDTA. The purified proteins and soluble fractions, together with soluble fractions of IPTG-induced bacteria, were boiled in Laemmli buffer and separated by SDS-PAGE. The purified protein fractions were also used in antibody blocking experiments.

Tissue Culture and DNA Transfection

HeLa cells were grown in DME supplemented with 10% FBS (Monteiro and Mical, 1996). Exponentially growing cells were transfected with 10–20 μg of plasmid DNAs as calcium phosphate precipitates (Graham and van der Eb, 1973).

Staining of Cells and Analysis by Immunofluorescence Light Microscopy

For immunofluorescence microscopy, cells were transfected directly on glass coverslips. At various times after transfection, the coverslips were fixed in 1% paraformaldehyde on ice for 15 min and then immersed in −20°C 70% ethanol for 20 min or overnight. The cells on the coverslips were rehydrated in PBS, blocked in 0.8% BSA, stained with primary and secondary antibodies, and finally stained with 1 μg/ml 4′6-diamidino-2-phenylindole (DAPI) as previously described (Monteiro et al., 1994). The primary antibodies used were the mouse monoclonal anti–myc 9E10 antibody (Monteiro et al., 1994), a goat polyclonal anti–PS-2 antibody generated using a 20-aa peptide corresponding to NH_2-terminal sequences for PS-2 (Santa Cruz Biotechnology, Inc., Santa Cruz, CA), a rabbit polyclonal anti-GFP antibody (CLONTECH Laboratories, Inc.), a rabbit polyclonal anticalreticulin (StressGen, Victoria, Canada), and a rabbit polyclonal antilamin antibody generated against purified bacterially expressed human lamin C. For antibody–ligand competition experiments, the goat anti–PS-2 antibody diluted 1:150 was incubated overnight with equal molar amounts (~250 μg) of either bacterially purified GST protein or the GST–NH_2-terminal PS-2 fusion protein before application to the transfected coverslips. Secondary antibodies used were affinity purified fluorescein- or rhodamine-conjugated rabbit anti–mouse, rabbit anti–goat, donkey anti–rabbit, donkey anti–goat, goat anti–mouse, and goat anti–rabbit antibodies (Jackson ImmunoResearch Laboratories, Inc., West Grove, PA). Fluorescence staining and phase contrast images of cells were visualized on an inverted Zeiss Axiovert 135 microscope (Thornwood, NY). Images were captured either on 35-mm TMAX 400 professional film (Eastman Kodak Corp., Rochester, NY), or using an Image Explorer II system incorporating a Dage MTI CCD72 camera and frame grabber together with IPLab Spectrum software (Signal Analytics Corp., Vienna, VA) on a Power Macintosh (Apple Computer Co., Cupertino, CA).

Analysis of GFP Fluorescence and Visual Monitoring of Cell Death

HeLa cells plated on gridded coverslips (Eppendorf, Milwaukee, WI) were transfected with GFP-expressing constructs, and at various times after transfection, the coverslips were washed with sterile PBS, and GFP fluorescence was visualized using the FITC filter 10 set (Carl Zeiss, Inc.). The fluorescence and phase contrast images of transfected cells in the same gridded areas were captured 17, 41, and 65 h after transfection using the Image explorer II camera. After image analysis, the PBS was replaced with fresh DMEM medium, and the coverslips were quickly returned to the CO_2 incubator.

In an alternative procedure, cell death was quantitated by counting the number of floating cells that accumulated 20 and 44 h after transfection. For this analysis, 1–1.5 × 10^5 HeLa cells grown in 100-mm dishes were transfected with either 15 or 20 μg DNA of the various PS-2 expression constructs. 20 h after transfection, the medium was collected from each dish and fresh medium was added to the dishes. The number of floating cells in medium obtained 20 and 44 h after transfection were counted using a hemacytometer. The number of floating apoptotic cells (of which 50–60% failed to exclude trypan blue—not untypical of apoptotic cells since loss of membrane integrity occurs very late during apoptosis) and not including mitotic cells (distinguished by the presence of metaphase plates) in the PS-2 transfected dishes were normalized to the number found in mock-transfected dishes.

Protein Preparation, SDS Gel Electrophoresis, and Immunoblotting

Cells were lysed in 0.5% SDS lysis buffer containing protease inhibitors (Monteiro and Mical, 1996) and the unboiled lysates were analyzed on 8.5 and 10% SDS-PAGE gels (Laemmli, 1970). The gels were calibrated by electrophoresing known molecular mass standards; rabbit muscle myosin (205 kD), *Escherichia coli* β-galactosidase (116 kD), rabbit muscle phosphorylase B (97.4 kD), bovine albumin (66 kD), egg albumin (45 kD), and carbonic anhydrase (29 kD) (Sigma Chemical Co.). The fractionated proteins were transferred onto 0.1-μm nitrocellulose membranes (Schleicher & Schuell, Keene, NH) by electroblotting, and immunoblots were processed as described previously (Xiao and Monteiro, 1994).

Double Labeling of PS-2–transfected HeLa Cells with the myc Monoclonal Antibody and Terminal Transferase Fluorescence In Situ Apoptosis Detection

Transfected cells were analyzed for apoptosis using the in situ Apop Tag detection kit (Oncor, Inc., Gaithersburg, MD) essentially as described by the manufacturer. HeLa cells transfected on coverslips were fixed in 1% paraformaldehyde on ice for 15 min, transferred to 0.5% Triton in PBS for 3 min, and placed in −20°C 70% ethanol for 20 min. The cells on coverslips were rehydrated by two incubations with PBS for 5 min each and then transferred to a humidified chamber and covered with Equilibration buffer (Oncor S7110 kit) for 5 min, after which the buffer was replaced with the working strength terminal deoxynucleotide transferase enzyme. The chamber containing the coverslips was placed in a 37°C incubator, and after 3.5 h, the coverslips were submerged in the working strength stop/wash buffer for 0.5 h and rinsed in three changes of PBS for 3 min each. Working strength antidigoxigenin-fluorescein was applied for 0.5 h, and the cells were washed again first in 1% Triton in PBS for 3 min and twice more in PBS for 5 min each. The coverslips were then counterstained with the myc monoclonal antibody followed by rhodamine-conjugated goat anti–mouse antibody as described above.

Results

The First 166 Residues of PS-2 Are Sufficient for ER Targeting

To investigate PS-2 function, full-length PS-2 and progressive COOH-terminal truncations, tagged at their COOH terminus with a myc epitope and under transcriptional control of a CMV promoter (Fig. 1), were expressed in HeLa cells by transient transfection. Immunoblot analysis of protein lysates prepared from cells transfected with either myc-tagged or nontagged full-length PS-2 contained immunoreactive bands of ~50–54 kD when probed with a polyclonal antibody specific for NH_2-terminal PS-2 sequences (Fig. 2 *C*, lanes *2* and *4*, respectively) that were not detectable in mock-transfected lysates (Fig. 2 *C*, lanes *1* and *3*). The PS-2 antibody recognized GST fusion proteins containing NH_2-terminal but not loop or COOH-terminal PS-2 sequences (Fig. 2, *A* and *B*). PS-2 deletions in which the COOH-terminal 180, 226, and 282 residues were removed (see Fig. 1 and Materials and Methods) migrated as doublet bands in SDS-PAGE gels (evident in shorter exposures of autoradiographs, data not shown) with apparent molecular sizes

of ~35–37, 33–35, and 31–33 kD, respectively (Fig. 2 *C*, lanes *4–7*). Apart from these bands, larger immunoreactive complexes were routinely seen in PS-2–transfected cells but not in mock-transfected cells and appeared to represent dimers, trimers, and higher molecular mass complexes of PS-2 proteins (Fig. 2 *C*, lanes *4–7*, *small arrowheads*). We did not observe any significant proteolytic cleavage of the PS-2–expressed products as has been previously reported (Kim et al., 1997; Tomita et al., 1997). In fact, immunoblot analyses of a parallel gel probed with the myc antibody, which recognized the COOH terminus of PS-2, contained bands identical in size to those recognized by the anti–NH_2-terminal PS-2 antibody, indicating full-length accumulation of the various PS-2 polypeptides with the presence of both NH_2- and COOH-terminal epitopes (compare Fig. 2 *C*, lanes *3–7*, with Fig. 2 *D*, lanes *1–5*). The myc-reactive PS-2 bands were clearly distinguished from the ~35 and 65 kD endogenous bands present in all HeLa cell lysates (Fig. 2 *D*, *small arrowhead*).

Immunofluorescence staining of HeLa cells transiently transfected with full-length myc-tagged PS-2 (pPS-2+Myc) displayed nuclear envelope and ER staining when probed with either the anti–NH_2-terminal PS-2 or myc antibodies (Fig. 3, *A* and *B*). In fact there was complete colocalization upon double staining with the two antibodies, corroborating the immunoblot data for lack of cleavage and separation of NH_2- and COOH-terminal PS-2 epitopes. The specificity of this double staining was demonstrated by preincubation of the PS-2 NH_2-terminal antibody with purified GST–PS-2 NH_2-terminal fusion protein (shown in Fig. 2 *A*, lane *6*), which abolished PS-2 NH_2-terminal staining almost completely, but myc staining was retained (Fig. 3, *C* and *D*, respectively). To confirm PS-2 was localized to the ER, we double stained transfected cells for calreticulin, a calcium-binding protein that is localized to the ER (Opas et al., 1991), and for PS-2 using the NH_2-terminal antibody. Full-length myc-tagged PS-2, as well as the three deletion constructs in which 180, 226, and 282 COOH-terminal PS-2 residues were deleted, showed colocalization with calreticulin (Fig. 3, *E–H* and data not shown). In contrast, construct pPS-2(138aa)+Myc, deleted of 310 COOH-terminal residues, including TMD2, did not show colocalization with calreticulin (Fig. 3, *I* and *J*). These results indicated that 166 NH_2-terminal residues of PS-2 are sufficient for ER tar-

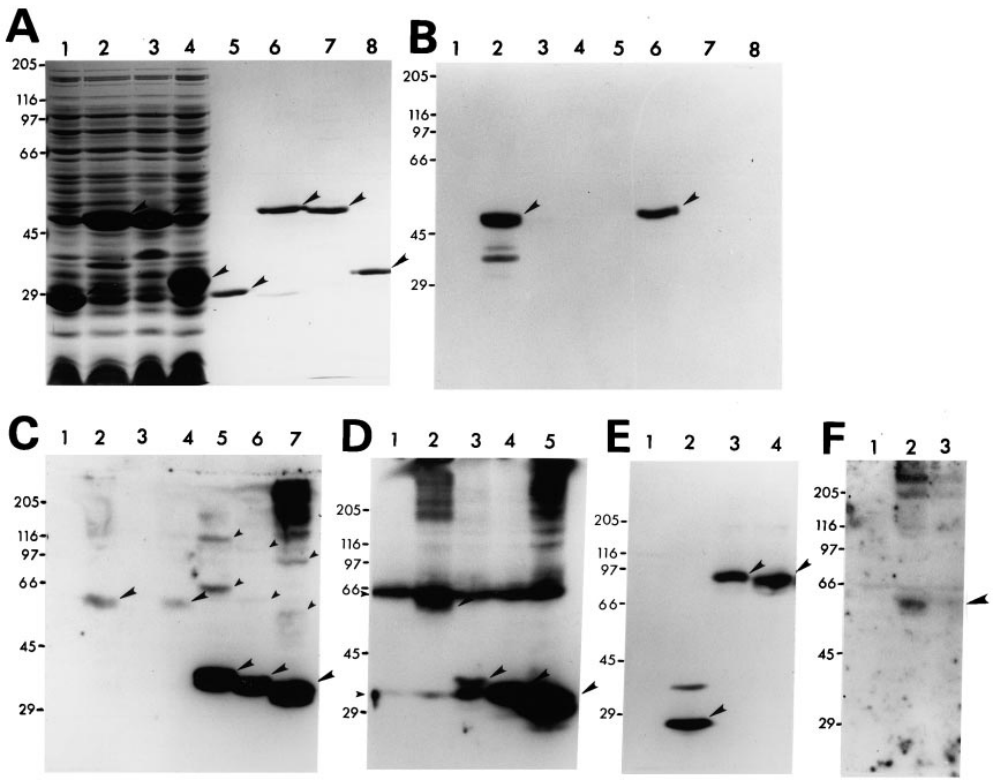

Figure 2. Immunoblot analysis of PS-2 proteins. (*A* and *B*) PS-2 NH_2-terminal, loop, and COOH-terminal sequences were expressed as GST fusion proteins and separated by SDS-PAGE on 8.5% polyacrylamide gels. The separated proteins were either stained with Coomassie blue (*A*) or transferred onto nitrocellulose filters and immunoblotted with the PS-2 NH_2-terminal antibody (*B*). Lanes *1–4* are whole cell lysates of bacteria induced for expression of GST fusion proteins by addition of IPTG, and lanes *5–8* are the corresponding purified GST fusion proteins. The GST fusion proteins that were expressed are as follows: Lanes *1* and *5*, GST alone; lanes *2* and *6*, GST–NH_2-terminal fusion protein; lanes *3* and *7*, GST–loop fusion protein; and lanes *4* and *8*, GST–COOH-terminal fusion protein. The *arrowheads* indicate the position of full-length GST fusion proteins. (*C–F*) Protein lysates of transfected HeLa cells separated by SDS-PAGE on 8.5% gels and immunoblotted with antibodies that recognize the transfected proteins. (*C*) Immunoblot with the anti–PS-2–specific antibody. Lanes *1–7* are lysates of cells transfected with the following constructs: Lanes *1* and *3*, mock-transfected cells; lane *2*, pPS-2; lane *4*, pPS-2+Myc; lane *5*, pPS-2(268aa)+Myc; lane *6*, pPS-2(222aa)+Myc; and lane *7*, pPS-2(166aa)+Myc. (*D*) Immunoblot of corresponding lysates shown in *C* with the anti-myc antibody. Lysates in lanes *1–5* in *D* correspond to lysates in lanes *3–7* in *C*. (*E*) Immunoblot with the anti–GFP-specific antibody. Lanes *1–4* are protein lysates of cells transfected with the following constructs: Lane *1*, mock-transfected cells (control); lane *2*, pGFP; lane *3*, pGFP–PS-2; and lane *4*, pGFP–PS-2(N141I). (*F*) Immunoblot of nonfusion PS-2 proteins with the NH_2-terminal PS-2 antibody. Lanes *1–3* are 100 μg of protein lysates of cells transfected with equivalent amounts of the following nonfusion PS-2 constructs: Lane *1*, mock-transfected; lane *2*, pPS-2 (wild-type); and lane *3*, pPS-2(Asn141Ile) mutant. The positions of protein molecular weight markers are indicated. Full-length PS-2 containing polypeptide bands seen only in transfected cell lysates are marked with large arrowheads. The small arrowheads indicate the positions of larger PS-2 complexes.

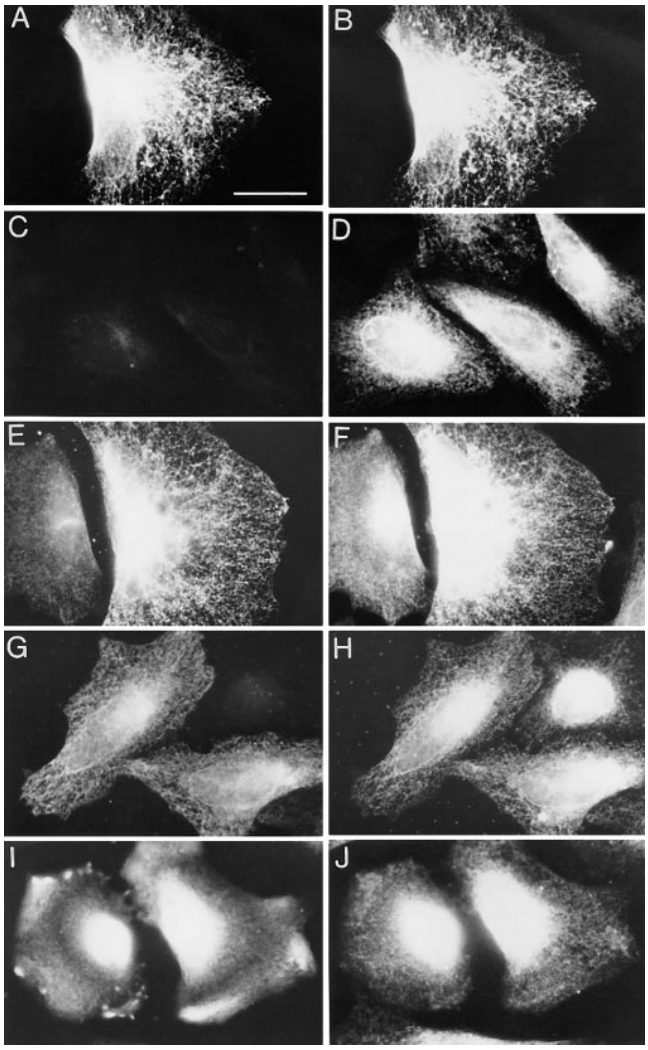

Figure 3. Immunofluorescence localization of PS-2 proteins in HeLa cells. (*A–D*) HeLa cells transiently transfected with PS-2+Myc and stained for PS-2 expression using antibodies specific for either the PS-2 NH_2 terminus (*A* and *C*) or the myc tag at the COOH terminus (*B* and *D*). The anti–PS-2 antibody was preincubated with either purified GST nonfusion protein for *A* and *B* or GST–NH_2-terminal fusion protein for *C* and *D* to demonstrate specificity of the anti–PS-2 NH_2-terminal antibody. Double staining of the transfected cells with the preincubated PS-2 and anti-myc antibodies demonstrate that staining is abolished only upon incubation with GST fusion proteins containing NH_2-terminal PS-2 sequences. Staining for both NH_2- and COOH-terminal epitopes showed complete colocalization (compare *A* and *B*), suggesting the two epitopes are not dissociated (not proteolytically cleaved and differentially localized). (*E–J*) HeLa cells transiently transfected with constructs pPS-2+Myc (*E* and *F*), pPS-2(166aa)+Myc (*G* and *H*), and pPS-2(138aa)+Myc (*I* and *J*) and double stained for PS-2 and calreticulin. The left and right panels show the same cells double-stained for either PS-2 expression, using the anti–NH_2-terminal PS-2 antibody (*E*, *G*, and *I*), or for endogenous calreticulin (*F*, *H*, and *J*). Please note complete colocalization of PS staining with calreticulin in pPS-2+Myc– and pPS-2(166aa)+Myc–expressing cells but not with pPS-2(138aa)+Myc–transfected cells. Bar, 10 μm.

geting. Since pPS-2(138aa)+Myc did not localize correctly to the ER, it was not studied further.

PS-2 Expression in HeLa Cells Causes Abnormal Nuclear Morphology

An obvious consequence of increased synthesis of PS-2 in transfected HeLa cells was the development of abnormal nuclear morphologies. An examination of PS-2 staining, DNA staining, and the phase contrast images of cells expressing full-length PS-2+myc and the three PS-2 deletion mutants 24 h after transfection, clearly revealed that PS-2 expression results in abnormal changes in nuclear shape (Fig. 4, *A–F*, and data not shown). For example, in Fig. 4 *A*, the two positively stained PS-2–transfected cells have condensed and shrunken nuclei compared to the untransfected cells in the same field. Interestingly, the change in nuclear morphology appeared to correlate with the amount of PS-2 protein expressed as revealed by differences in the staining intensity. These features were consistently seen in PS-2–overexpressing cells but not in mock-transfected controls and HeLa cells transfected with lamin or potassium channel cDNAs (Fig. 4, *G–I*). The overt changes in nuclear morphology were therefore not simply due to the overexpression of a protein targeted to the nuclear envelope, as in the case of lamins, or a transmembrane protein since the Kv1.4 channel has almost the same number of transmembrane domains and has a general topology to that of the presenilins (see Fig. 1).

The rate at which nuclear changes became apparent was construct dependent, with pPS-2+Myc, pPS-2(268aa)+Myc, and pPS-2(222aa)+Myc all causing more rapid changes than pPS-2(166aa)+Myc–transfected cells. This time-dependent change in nuclear morphology correlated with an increase in floating dead cells in the medium. Quantification of the rate of cell death induced by the different PS-2 constructs 20 and 44 h after transfection revealed that pPS-2+Myc, pPS-2(268aa)+Myc, and pPS-2(222aa)+Myc kill cells at similar rates (Fig. 5 *A*). In contrast, in cells transfected with PS-2(166aa)+Myc this rate was reduced ~70% 20 h after transfection, but by 44 h it had accelerated and approached that of the other constructs (Fig. 5 *A*).

Abnormal Nuclear Morphology as a Consequence of PS-2 Expression Correlates with Death of HeLa Cells by Apoptosis

The striking changes seen in PS-2–transfected cells were reminiscent of the nuclear and morphological changes that occur during programmed cell death, or apoptosis (Wyllie, 1980; Earnshaw, 1995). To investigate if the cells were indeed dying by apoptosis, we used the terminal deoxynucleotide transferase nick end labeling (TUNEL) assay to identify apoptotic cells. HeLa cells transfected with pPS-2(166aa)+Myc offered an unusual opportunity to determine if the putative dying cells could be TUNEL labeled since they manifested and displayed the morphological features of apoptosis over a prolonged time period and the expressed cells adhered to the coverslips up until 40 h after transfection. In contrast, we were unable to TUNEL label cells transfected with full-length PS-2 since most of the transfected cells had lifted off of the coverslips by 18–24 h after transfection, probably as a consequence of a faster

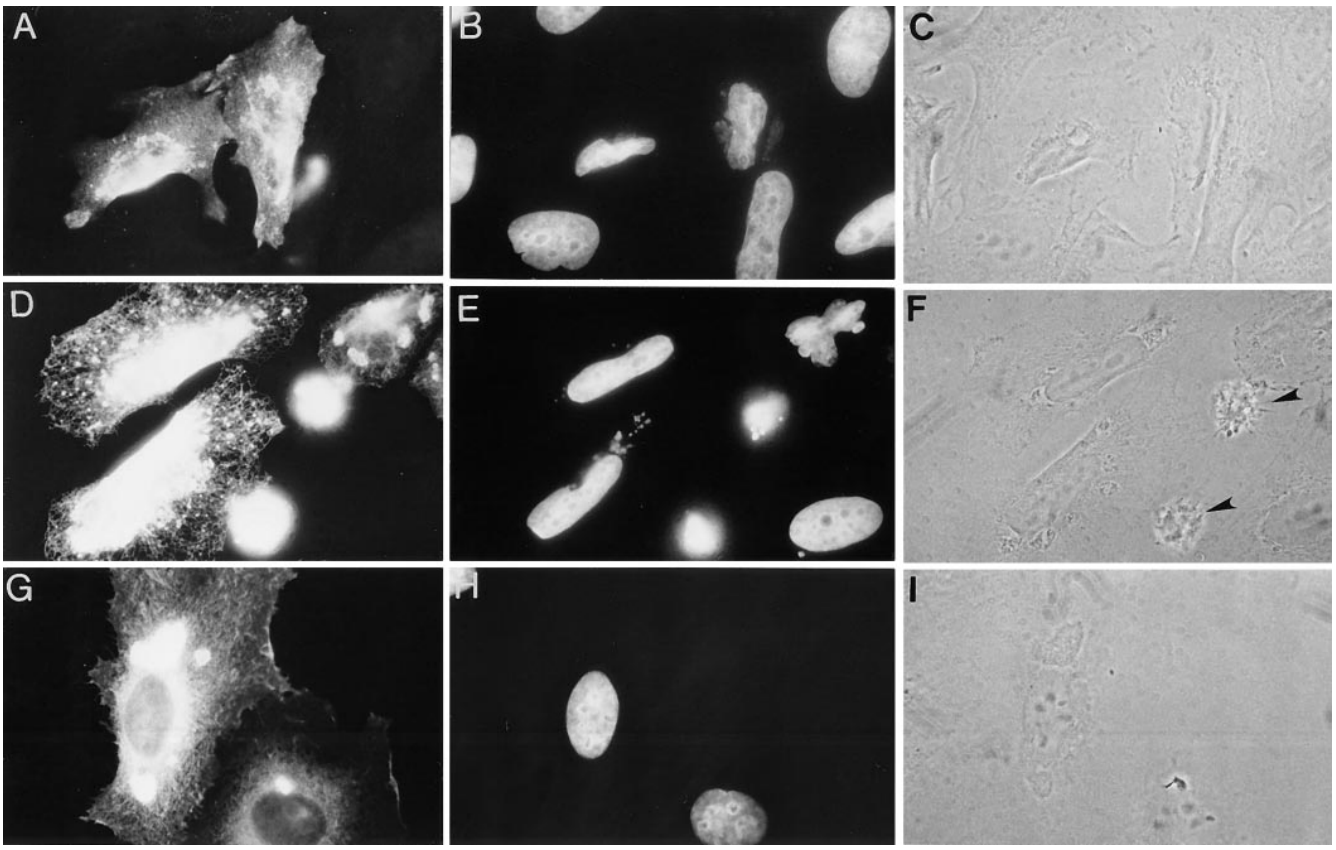

Figure 4. Overexpression of PS-2 proteins in HeLa cells leads to overt changes in nuclear morphology. HeLa cells were transfected with pPS-2+Myc (*A–C*), pPS-2(268aa)+Myc (*D–F*), or pKv1.4+Myc (*G–I*). (*A*, *D*, and *G*) Anti-myc staining of cells 24 h after transfection. The center panels are the corresponding DNA images of the cells revealed by DAPI staining, and the right panels are the phase contrast images of the same cells. Please note that the majority of cells expressing high levels of PS-2 have dismorphic nuclei. In some of these cells, the nuclei are highly condensed with rounded-up and shrunken cytoplasms (*arrowheads*).

death rate and the multiple washing steps used in the TUNEL assay.

Fig. 6, *A–D*, shows a typical example of PS-2(166aa)+Myc–transfected cells in which TUNEL-positive labeling (Fig. 6 *B*) correlated with PS-2 expression (Fig. 6 *A*). Interestingly, only the highly condensed nuclei of the rounded-up shrunken cells that appear about to detach from the coverslip (seen by the phase contrast image; Fig. 6 *D*, *arrowheads*) were prominently labeled. Even the PS-2–positive cell with the multiple compacted DNA aggregates, seen by DAPI staining (Fig. 6 *C*), was not TUNEL labeled, suggesting that it is an earlier stage of apoptosis during which few free DNA 3′ ends have been generated or are accessible for labeling. In addition to DNA cleavage, another feature of cells undergoing apoptosis is the collapse of the nuclear envelope and cleavage of lamin proteins (Kaufmann, 1989; Ucker et al., 1992; Oberhammer et al., 1994; Lazebnik et al., 1995; Rao et al., 1996). We therefore examined the integrity of the nuclear lamina in pPS-2 (166aa+Myc–transfected cells using an antibody specific for lamins A/C (Fig. 6, *E–H*). In PS-2–expressing cells, the nuclear lamina had indeed collapsed but was round and apparently normal in PS-2–negative cells. In some PS-expressing cells, the nuclear lamina was diffuse, suggesting cleavage of the nuclear lamins during apoptosis.

Direct Demonstration that Overexpression of PS-2 Causes Cell Death Using GFP as a Reporter

To directly watch temporally the pathway of apoptosis, we generated GFP fusion proteins in which PS-2 was fused in frame to the COOH terminus of the GFP. Two different constructs were studied. The first was pGFP–PS-2, in which wild-type PS-2 was linked to GFP. The second was pGFP–PS-2(N141I), containing the AD-associated PS-2 mutation at codon 141, converting asparagine to isoleucine (Levy-Lahad et al., 1995*a*; Rogaev et al., 1995). Immunoblot analysis of transfected HeLa cell lysates indicated both GFP–PS-2 fusion proteins to migrate on SDS-PAGE as ~80-kD polypeptides (Fig. 2 *E*), consistent with fusion of 27 kD of GFP sequences with 50–55 kD of PS-2. There was no evidence for any proteolytic cleavage of the fusion proteins. Furthermore, both GFP–PS-2 fusion proteins displayed classical ER and nuclear envelope localization when examined by direct fluorescence microscopy (Fig. 7, *A* and *B*), indicating that fusion of GFP with PS-2 did not noticeably alter the normal ER localization pattern of PS-2.

HeLa cells grown on gridded coverslips were transfected with the GFP vector lacking any insert or with the GFP–PS-2 fusion constructs, and the effects on cell viability were studied over time. Images of cells on different coverslip ar-

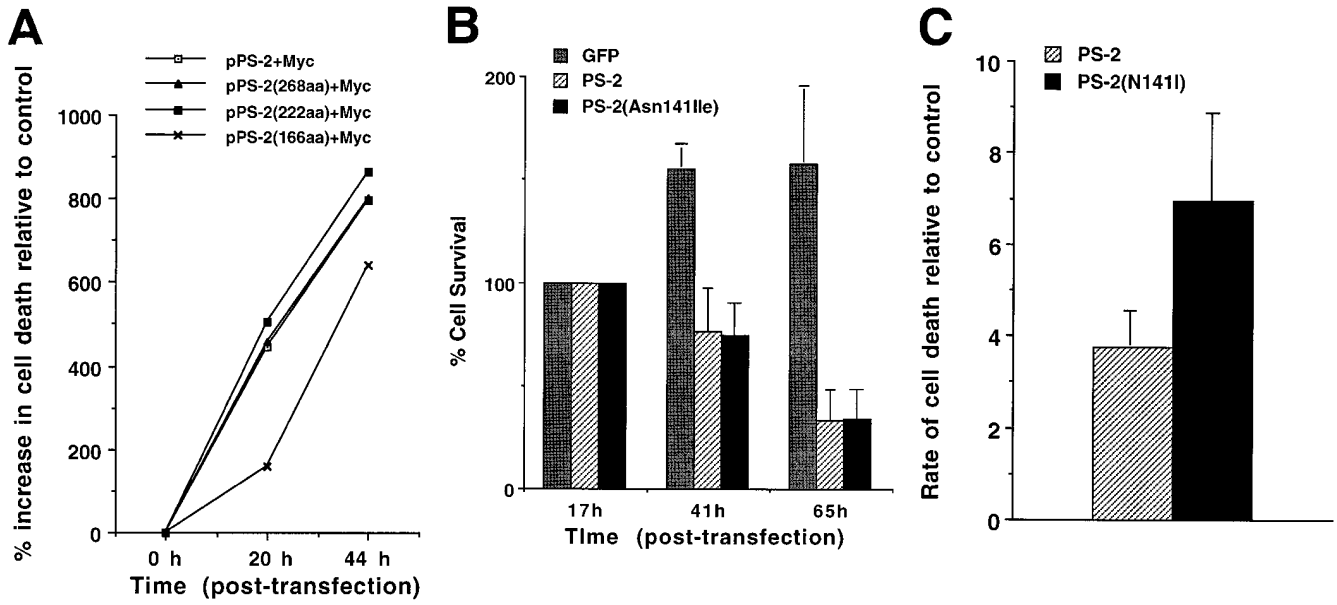

Figure 5. Quantitation of cell survival upon transfection of PS-2 constructs. (*A*) HeLa cells were transfected with 20 μg equivalents of pPS-2+Myc, pPS-2(268aa)+Myc, pPS-2(222aa)+Myc, or pPS-2(166aa)+Myc DNAs or were mock transfected, and the number of floating cells that accumulated in the media were counted 20 and 44 h after transfection. The line graph shows the number of floating cells (dead cells) in four separate experiments relative to that seen in control mock-transfected cells. The average error for four experiments was ~10–15% and is not included for clarity of presentation. Note, cells transfected with pPS-2(166aa)+Myc DNA displayed delayed cell death at 20 h. (*B*) HeLa cells were transfected with either pGFP, pGFP-PS-2, or pGFP-PS-2(N141I), and fluorescent images of the same coverslip areas were captured and counted 17, 41, and 65 h after transfection. The number of fluorescent cells seen at 41 and 65 h were normalized to the numbers seen at 17 h as a means of measuring the effects of expression of the GFP constructs on cell viability. The histograms show the average percentage of cell viability in six independent transfections with the GFP–PS-2 and GFP–PS-2(Ans141Ile) constructs, and the corresponding average for three transfections with the GFP construct. (*C*) HeLa cells were transfected with equivalent amounts plasmid DNA expressing either wild-type PS-2 or PS-2 containing the AD-associated mutation (N141I). The number of dead cells was counted 40 h after transfection. The histogram shows the rates of cell death in three separate experiments using 15 μg of plasmid DNA relative to the number of dead cells found in the mock-transfected controls.

eas were recorded 17 h after transfection, and the same areas (identified by grid markings on the coverslips) were reexamined 41 and 65 h after transfection (examples of such fields are shown in Fig. 7 *B*). The number of fluorescing cells seen 41 and 65 h after transfection were normalized to the cell counts at 17 h. As shown in Fig. 5 *B*, the number of cells expressing GFP increased ~155% after 41 h and to 158% at 65 h. The initial increase at 41 h probably resulted from either cell division of the transfected cells (the HeLa cell cycle is ~23 h; Monteiro and Mical, 1996) and/or an increase in GFP expression in cells previously scored as nonexpressors. The smaller increase at 65 h is probably due to loss of transient GFP expression during prolonged growth. In sharp contrast, cell viability dramatically decreased in cells expressing GFP–PS-2 fusion proteins. 41 h after transfection, cell viability decreased to ~76% in cells expressing wild-type PS-2 fusion proteins and decreased further to 33% by 65 h. A similar dramatic decrease in cell viability was seen in cells expressing the PS-2(N141I) mutation with viability decreasing to 74% at 41 h and 38% after 65 h. In both cases, decrease in cell viability correlated with the appearance of numerous rounded-up shrunken cells at the later time points, consistent with cell death by apoptosis. However, a careful comparison of cell viability in six sets of independent experiments and analysis of greater than 2,000 cells indicated no significant difference in the rate of cell survival between wild-type and mutant PS-2 GFP fusion proteins in HeLa cells (Fig. 5 *B*).

The time-dependent loss of GFP fluorescence could have resulted from the loss of transient expression or the loss of cells from the coverslips due to death. To test these and other possibilities, we followed individual GFP-expressing cells over a period of time. A typical example of this analysis is shown in Fig. 8, where at least three of a group of cells attached on the No. 2 grid mark of the coverslip are clearly seen to express the GFP–PS-2 fusion protein by fluorescence at 22 h. After 50 h, these same cells, which had retained some residual fluorescence, had rounded-up and had shrunken cytoplasms typical of dying cells.

A Comparison of Nonfusion PS-2 Proteins Indicates the AD-associated (Asn141Ile) Mutation Increases Cell Death

The lack of a noticeable difference in the rate of cell survival between wild-type PS-2 and the AD-associated mutation when studied as GFP fusion proteins could have resulted from the GFP moiety masking or interfering with PS-2 properties. Therefore, wild-type and the AD PS-2 mutant were expressed and studied as nonfusion proteins in HeLa cells by transient transfection of equivalent amounts of DNA. Measurement of dead floating cells 40 h after

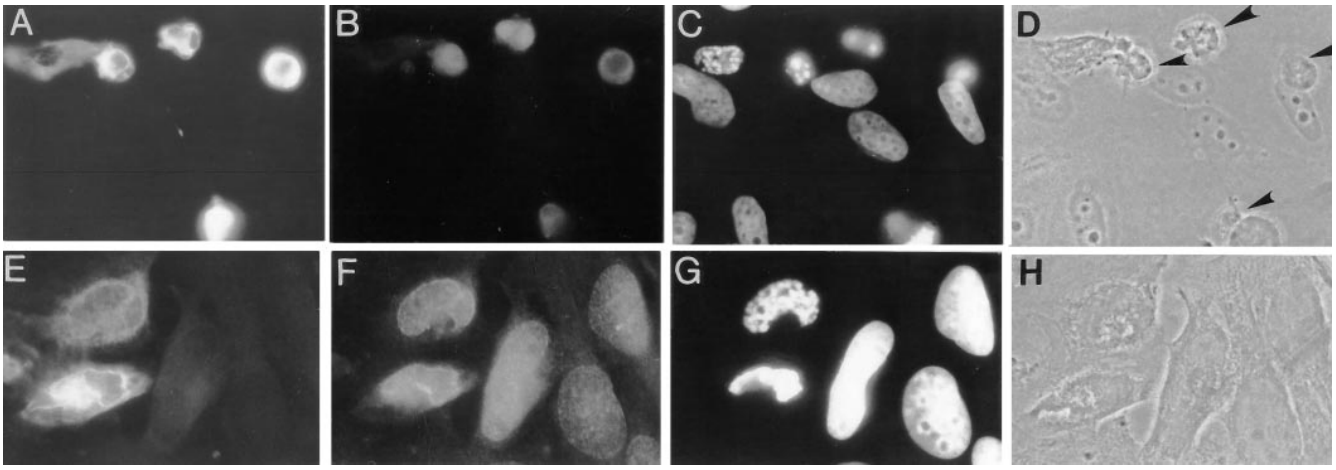

Figure 6. Correlation of apoptotic events in HeLa cells expressing PS-2. HeLa cells were transfected with the pPS-2(166aa)+Myc construct and were examined for apoptotic or morphological changes 48 h after transfection. The rows of panels are the same cells stained for PS-2 protein (*A* and *E*), TUNEL labeling (*B*), or lamin staining (*F*); DAPI staining of DNA (*C* and *D*) and phase contrast images (*D* and *H*). Cells that labeled positive for TUNEL appeared rounded-up and shrunken by phase contrast microscopy (*arrowheads*).

transfection indicated the mutant kills cells 1.84-fold faster than does wild-type PS-2 (Fig. 5 *C*). Since the cells were dying at different rates it was difficult to normalize transfection efficiencies using unlinked reporters. However, the mutant may be considerably more toxic than was estimated by our experiments if less mutant DNA was transfected since immunoblotting of equivalent protein lysates, prepared from parallel sets of transfections 20 h after transfection, indicated the mutant to be expressed ~25% that of wild-type protein levels (Fig. 1 *F*).

Discussion

The evidence presented here demonstrates that forced expression of PS-2 in HeLa cells, by itself, is sufficient to induce apoptosis and that the AD-associated mutation N141I induces an increase in cell death. Initially, it was thought that PS-2 may inhibit apoptosis because a COOH-terminal fragment of mouse PS-2, termed ALG-3, rescued T cells from receptor-induced programmed cell death (Vito et al., 1996*a*). More recently, the cause of this rescue has been shown to be an artifactual consequence of expressing a PS-2 fragment such that it acts in a dominant negative fashion (Vito et al., 1996*b*). Further evidence supporting the participation of PS-2 in apoptosis was obtained upon expression of either wild-type or mutant PS-2(N141I) in PC12 cells that had been triggered by external stimuli to undergo apoptosis (Deng et al., 1996; Wolozin et al., 1996). PS-2 expression accelerated death in these cells, with the PS-2(N141I) mutant increasing apoptosis but only in cells grown under certain culture conditions (Wolozin et al., 1996). The PC12 studies offered only weak evidence for the apoptotic property of PS-2 since the cells had been primed to undergo apoptosis by external agents. Moreover, PC12 cells are balanced at a suicidal decision and are particularly susceptible to induction of apoptosis by a wide variety of stimuli. Our results showing apoptotic induction in HeLa cells provide strong and independent evidence for the PS-2 apoptotic property since HeLa cells are typically highly resistant to apoptosis.

The mechanisms by which PS-2 overexpression leads to cell death by apoptosis are not revealed by our studies. Although the presenilins are ubiquitously expressed, PS-2 is expressed at considerably lower levels than PS-1 (Rogaev et al., 1995; Sherrington et al., 1995; Li et al., 1995; Lee et al., 1996). Perhaps in normal cells, expression of one or both of the presenilins is modulated by other factors that regulate the commitment to the cell death pathway. Presumably, in the transient transfections increases in expression of PS-2 leads to the perturbation of this regulation in favor of the apoptotic pathway.

Although PS-1 is highly homologous to PS-2, no increased apoptosis has been documented in cell lines and transgenic mice overexpressing PS-1 (Duff et al., 1996; Kovacs et al., 1996; Thinakaran et al., 1996). While the simplest explanation is that PS-1 may function differently from PS-2, another possibility is that transgenic lines overexpressing PS-1 may induce compensatory changes in the expression of antiapoptotic genes. Another likely possibility is that proteolytic cleavage of PS proteins alter their properties significantly. Most prior reports have shown overexpression of PS proteins in cell lines and transgenic mice to yield primarily proteolytic products. However, in our experiments we failed to observe significant cleavage (<5–10%) of the expressed PS-2 proteins, including those containing full-length PS-2 sequences. Based on these observations, we propose that proteolytic cleavage of the presenilins diminishes the apoptotic effects of the full-length proteins. That PS truncations are less toxic than full-length proteins is supported by higher levels of truncated proteins that accumulated with increasing length of COOH-terminal truncations (see Fig. 2, *C* and *D*).

The AD-associated PS-2 mutation converting arginine to isoleucine at codon 141 caused an increase in apoptosis in cells overexpressing the mutant protein. Despite accumulating to lower protein levels than the wild-type protein, the mutant is more toxic. The deletion studies pre-

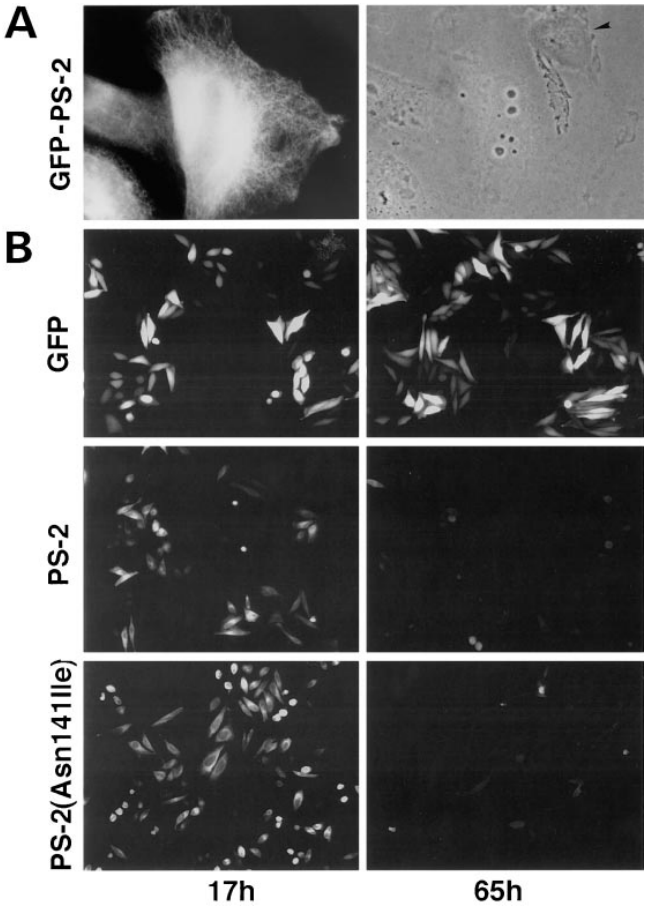

Figure 7. Fluorescent studies of PS-2 expression in HeLa cells using GFP as a reporter. (*A*) Fluorescent and phase contrast images of living HeLa cells transfected with pGFP–PS-2, showing the GFP–PS-2 fusion protein is localized to the ER. A presumably untransfected cell is indicated by the arrowhead. (*B*) HeLa cells were transfected with either GFP alone (*top row*), GFP fused with wild-type PS-2 (*second row*), or GFP fused with the AD PS-2(N141I) mutant (*bottom row*). The fluorescent images of cells expressing GFP proteins on the same area of the gridded coverslip were captured 17 and 65 h after transfection. Please note, the number of fluorescing cells 65 h after transfection increases in cells expressing GFP alone, whereas cells expressing the two GFP–PS-2 fusion constructs show a dramatic decrease in fluorescence.

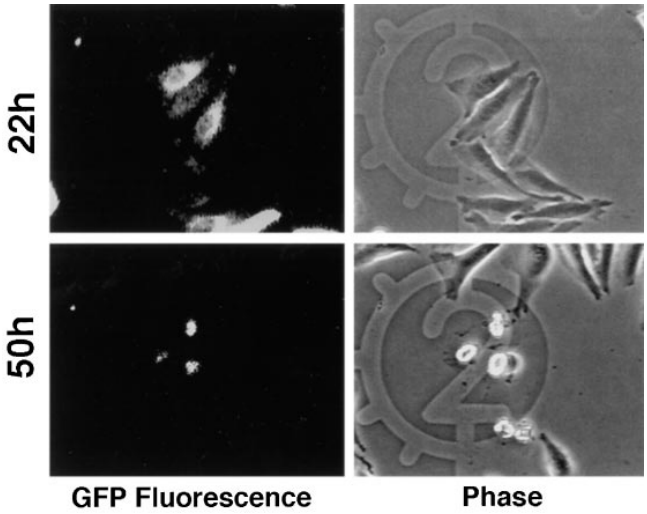

Figure 8. Direct demonstration that PS-2 overexpression in HeLa cells causes cell death. HeLa cells were transfected with a GFP–PS-2 fusion construct, and images of an individual group of transfected cells on the No. 2 region of the gridded coverslip were recorded at various times after transfection. The GFP fluorescent (*left*) and phase contrast images (*right*) of the same coverslip region 22 and 50 h after transfection are shown. By following this group of cells it was possible to conclude that the same three cells expressing the GFP fusion protein at 22 h had rounded-up and died by 50 h.

sented here have indicated that retention of NH_2-terminal PS-2 sequences are necessary for apoptosis. Not surprisingly, fusion of GFP to the NH_2 terminus of PS-2 masks these differences.

Clearly, if the differential killing effect of full-length wild-type and mutant PS-2 is relevant to disease, then it must manifest in neurons that are at risk in AD. Suggestive evidence that apoptosis may be involved in AD is supported by increased accumulation of the death-promoting protein, Bax, as well as increased evidence for nuclear DNA fragmentation, in AD cases but not in controls (Su et al., 1997). Additionally, recent reports suggest that AD mutations in βAPP may also induce apoptosis when expressed in neuronal cells and that death is mediated by heterotrimeric guanosine triphosphate–binding proteins (G proteins; Yamatsuji et al., 1996). Interestingly, FAD patients with mutations in presenilin genes and transgenic mice expressing mutant human PS genes have elevated levels of Aβ42-43 peptides (Duff et al., 1996; Scheuner et al., 1996; Borchelt et al., 1996; Tomita et al., 1997), which have been documented to induce apoptosis (LaFerla et al., 1995). The obvious implications of all of this is that missense mutations in presenilins produce subtle effects that increase apoptosis over the course of the neuronal life span.

We gratefully acknowledge the help of Weihong Zha and Meredith Hopkins in constructing the PS-2 Bluescript and pGFP-PS-2(Δ86aa) constructs, respectively. We thank Dr. Ann Pluta and a benevolent reviewer for *The Journal of Cell Biology* for insightful comments on the manuscript.

This work was supported in part by a grant from the National Institute on Aging to M.J. Monteiro.

Received for publication 28 April 1997 and in revised form 19 August 1997.

References

Alzheimer's Disease Collaborative Group. 1995. The structure of the presenilin 1 (S182) gene and identification of six novel mutations in early onset AD families. *Nat. Genet.* 11:219–222.

Borchelt, D.R., G. Thinakaran, C.B. Eckman, M.K. Lee, F. Davenport, T. Ratovitsky, C.-M. Prada, G. Kim, S. Seekins, D. Yager, et al. 1996. Familial Alzheimer's disease-linked presenilin 1 variants elevate Aβ1-42/1-40 ratio in vitro and in vivo. *Neuron.* 17:1005–1013.

Boteva, K., M. Vitek, H. Mitsudade, H. Silva, P.-T. Xu, G. Small, and J.R. Gilbert. 1996. Mutation analysis of presenilin 1 gene in Alzheimer's disease. *Lancet.* 347:130–131.

Campion, D., J.M. Flaman, A. Brice, D. Hannequin, B. Dubois, C. Martin, V. Moreau, F. Charbonnier, O. Didierjean, S. Tardieu, et al. 1995. Mutations in the presenilin 1 gene in families with early-onset Alzheimer's disease. *Hum. Mol. Genet.* 4:2373–2377.

Chapman, J., A. Asherova, N. Wang, T.A. Treves, A.D. Korczyn, and L.G. Goldfarb. 1995. Familial Alzheimer's disease associated with S182 codon 286 mutation. *Lancet.* 346:1040.

Cook, D.B., J.C. Sung, T.E. Golde, K.M. Felsenstein, B.S. Wojczyk, R.E. Tanzi, J.Q. Trojanowski, V.M.Y. Lee, and R.M. Doms. 1996. Expression and analy-

sis of presenilin-1 in a human neuronal system: localization in cell bodies and dendrites. *Proc. Natl. Acad. Sci. USA*. 93:9223–9228.
Corder, E.H., A.M. Saunders, W.J. Strittmatter, D.E. Schmechel, P.C. Gaskell, G.W. Small, A.D. Roses, J.L. Haines, and M.A. Pericak-Vance. 1993. Gene dose apolipoprotein E type 4 allele and the risk of Alzheimer's disease in late onset families. *Science (Wash. DC)*. 261:921–923.
Cruts, M., H. Backhovens, S.Y. Wang, G. Vangassen, J. Theurns, C. Dejonghe, A. Wehnert, J. Devoecht, G. deWinter, P. Cras, et al. 1995. Molecular genetic analysis of familial early-onset Alzheimer's disease linked to chromosome 14Q24.3. *Hum. Mol. Genet.* 4:2363–2371.
Cruts, M., L. Hendriks, and C. Van Broeckhoven. 1996. The presenilin genes: a new gene family involved in Alzheimer's disease pathology. *Hum. Mol. Genet.* 5:1449–1455.
Deng, G., C.J. Pike, and C.W. Cotman. 1996. Alzheimer-associated presenilin-2 confers increased sensitivity to apoptosis in PC12 cell. *FEBS Lett.* 397:50–54.
Doan, A., G. Thinakaran, D.R. Borchelt, H.H. Slunt, T. Rativitsky, M. Podlisny, D.J. Selkoe, M. Seeger, S.E. Gandy, D.L. Price, and S.S. Sisodia. 1996. Protein topology of presenilin 1. *Neuron.* 17:1023–1030.
Duff, K., C. Eckman, C. Zehr, X. Yu, C.-M. Prada, J. Perez-tur, M. Hutton, L. Buee, Y. Harigaya, D. Yager, et al. 1996. Increased amyloid-β42(43) in brains of mice expressing mutant presenilin 1. *Nature (Lond.)*. 383:710–713.
Earnshaw, W.C. 1995. Nuclear changes in apoptosis. *Curr. Opin. Cell Biol.* 7: 337–343.
Graham, R., and A.J. van der Eb. 1973. A new technique for the assay of infectivity of human adenovirus 5 DNA. *Virology.* 52:456–467.
Haass, C. 1997. Presenilins: genes for life and death. *Neuron.* 18:687–690.
Haass, C., Y. Hung, M. Citron, D.B. Teplow, and D.J. Selkoe. 1995. β-Amyloid, protein processing and Alzheimer's disease. *Drug Res.* 45:398–402.
Kaufmann, S.H. 1989. Induction of endonucleolytic DNA cleavage in human acute myelogenous leukemia cells by etoposide, camptothecin, and other cytotoxic anticancer drugs: a cautionary note. *Cancer Res.* 49:5870–5878.
Kim, T.W., W.H. Pettingell, O.G. Hallmark, R.D. Moir, W. Wasco, and R.E. Tanzi. 1997. Endoproteolytic cleavage and proteosomal degradation of presenilin 2 transfected cells. *J. Biol. Chem.* 272:11006–11010.
Kovacs, D.M., H.J. Fausett, K.J. Page, T.-W. Kim, R.D. Moir, D.E. Merriam, R.D. Hollister, O.G. Hallmark, R. Mancini, K.M. Felsenstein, et al. 1996. Alzheimer-associated presenilins 1 and 2: neuronal expression in brain and localization to intracellular membranes in mammalian cells. *Nat. Med.* 2: 224–229.
LaFerla, F.M., B.T. Tinkle, C.J. Bieberich, C. Haudenschild, and G. Jay. 1995. The Alzheimer's Aβ peptide induces neurodegeneration and apoptotic cell death in transgenic mice. *Nat. Genet.* 9:21–30.
Laemmli, U.K. 1970. Cleavage of structural proteins during the assembly of the head of bacteriophage T4. *Nature (Lond.)*. 227:680–685.
Lazebnik, Y.A., R. Takahashi, R. Moir, R. Goldman, G. Poirier, S. Kaufmann, and W. Earnshaw. 1995. Studies of lamin proteinase reveal multiple parallel pathways during apoptotic execution. *Proc. Natl. Acad. Sci. USA*. 92:9042–9046.
Lee, M.K., Z. Xu., P.C. Wong, and D.W. Cleveland. 1993. Neurofilaments are obligate heteropolymers in vivo. *J. Cell Biol.* 122:1337–1350.
Lee, M.K., H.H. Slunt, L.J. Martin, G. Thinakaran, G. Kim, S.E. Gandy, M. Seeger, E. Koo, D.L. Price, and S.S. Sisodia. 1996. Expression of presenilin 1 and 2 (PS1 and PS2) in human and murine tissues. *J. Neurosci.* 16:7513–7525.
Lehmann, S., R. Chiesa, and D.A. Harris. 1997. Evidence for a six-transmembrane domain structure of presenilin 1. *J. Biol Chem.* 272:12047–12051.
Levitan, D., and I. Greenwald. 1995. Facilitation of lin-12-mediated signalling by sel-12, a *Caenorhabditis elegans* S182 Alzheimer's disease gene. *Nature (Lond.)*. 377:351–354.
Levitan, D., T.G. Doyle, D. Brousseau, M.K. Lee, G. Thinakaran, H.H. Slunt, S.S. Sisodia, and I. Greenwald. 1996. Assessment of normal and mutant human presenilin function in *Caenorhabditis elegans. Proc. Natl. Acad. Sci. USA*. 93:14940–14944.
Levy-Lahad, E., W. Wasco, P. Poorkaj, D.M. Romano, J. Oshima, W.H. Pettingell, C. Yu, P.D. Jondro, S.D. Schmidt, K. Wang, et al. 1995*a*. Candidate gene for the chromosome 1 familial Alzheimer's disease locus. *Science (Wash. DC)*. 269:973–977.
Levy-Lahad, E., E.M. Wijsman, E. Nemens, L. Anderson, K.A.B. Goddard, J.L. Weber, T.D. Bird, and G.D. Schellenberg. 1995*b*. A familial Alzheimer's disease locus on chromosome 1. *Science (Wash. DC)*. 269:970–973.
Li, X., and I. Greenwald. 1996. Membrane topology of the *C. elegans* SEL-12 presenilin. *Neuron.* 17:1015–1021.
Li, J., J. Ma, and H. Potter. 1995. Identification and expression analysis of a potentially familial Alzheimer disease gene on chromosome 1 related to AD3. *Proc. Natl. Acad. Sci. USA*. 92:12180–12184.
Mercy, M.R., J.C. Troncoso, and M.J. Monteiro. 1992. A new series of trpE vectors that enable high expression of nonfusion proteins in bacteria. *Protein Expr. Purif.* 3:57–64.
Monteiro, M.J., and T. Mical. 1996. Resolution of kinase activities during the HeLa cell cycle: identification of kinases with cyclic activities. *Exp. Cell Res.* 223:443–451.
Monteiro, M.J., C. Hicks, L. Gu, and S. Janicki. 1994. Determinants for intracellular sorting of cytoplasmic and nuclear intermediate filaments. *J. Cell Biol.* 127:1327–1343.
Mullan, M., and F. Crawford. 1993. Genetic and molecular advances in Alzheimer's disease. *Trends Neurosci.* 16:398–403.
Oberhammer, F.A., K. Hochegger, G. Froschl, R. Tiefenbacher, and M. Pavelka. 1994. Chromatin condensation during apoptosis is accompanied by degradation of lamin A+B, without enhanced activation of cdc2 kinase. *J. Cell Biol.* 126:827–837.
Opas, M., E. Dziak, L. Fliegel, and M. Michalak. 1991. Regulation of expression and intracellular distribution of calreticulin, a major calcium binding protein of nonmuscle cells. *J. Cell Physiol.* 149:160–171.
Perez-Tur, J., S. Froelich, G. Prihar, R. Crook, M. Baker, K. Duff, M. Wragg, F. Busfield, C. Lendon, R.F. Clark, et al. 1995. A mutation in Alzheimer's disease destroying a splice acceptor site in the presenilin-1 gene. *Neuroreport.* 7:297–301.
Rao, L., D. Perez, and E. White. 1996. Lamin proteolysis facilitates nuclear events during apoptosis. *J. Cell Biol.* 135:1441–1455.
Rogaev, E.I., R. Sherrington, E.A. Rogaeva, G. Levesque, M. Ikeda, Y. Liang, H. Chi, C. Lin, K. Holman, T. Tsuda, et al. 1995. Familial Alzheimer's disease in kindereds with missense mutations in the gene on chromosome 1 related to the Alzheimer's disease type 3 gene. *Nature (Lond.)*. 376:775–778.
Scheuner, D., C. Eckman, X. Song, M. Citron, N. Suzuki, T.D. Bird, J. Hardy, M. Hutton, W. Kukull, E. Larson, et al. 1996. Secreted amyloid β-protein similar to that in the senile plaques of Alzheimer's disease is increased in vivo by the presenilin and 2 and APP mutations linked to familial Alzheimer's disease. *Nat. Med.* 2:864–870.
Shen, J., R.T. Bronson, D.F. Chen, W. Xia, D.J. Selkoe, and S. Tonegawa. 1997. Skeletal and CNS defects in presenilin-1-deficient mice. *Cell.* 89:629–639.
Sherrington, R., E.I. Rogaev, Y. Liang, E.A. Rogaeva, G. Levesque, M. Ikeda, H. Chi, C. Lin, G. Li, K. Holman, et al. 1995. Cloning of a gene bearing missense mutations in early-onset familial Alzheimer's disease. *Nature (Lond.)*. 375:754–760.
Sherrington, R., S. Froelich, S. Sorbi, D. Campion, H. Chi, E.A. Rogaeva, G. Levesque, E.I. Rogaev, C. Lin, Y. Liang, et al. 1996. Alzheimer's disease associated with mutations in presenilin 2 is rare and variably penetrant. *Hum. Mol. Genet.* 5:985–988.
Strittmatter, W.J., and A.D Roses. 1995. Apolipoprotein E and Alzheimer disease. *Proc. Natl. Acad. Sci. USA*. 92:4725–4727.
Su, J.H., G. Deng, and C.W. Cotman. 1997. Bax protein expression is increased in Alzheimer's brain: correlation with DNA damage, Bcl-2 expression, and brain pathology. *J. Neuropathol. Exp. Neurol.* 56:86–93.
Tamkun, M.M., K.M. Knoth, J.A. Wabridge, H. Kroemer, D.M. Roden, and K.M. Glover. 1991. Molecular cloning and characterization of two voltage-gated K channel cDNAs from human ventricle. *FASEB (Fed. Am. Soc. Exp. Biol.) J.* 5:331–337.
Thinakaran, G., D.R. Borchelt, M.K. Lee, H.H. Slunt, L. Spitzer, G. Kim, T. Ratovitsky, F. Davenport, C. Nordstedt, M. Seeger, et al. 1996. Endoproteolysis of presenilin 1 and accumulation of processed derivatives in vivo. *Neuron.* 17:181–190.
Tomita, T., K.. Maruyama, T.C. Saido, H. Kume, K. Shinozaki, S. Tokuhiro, A. Capell, J. Walter, H. Grunberg, C. Hass, et al. 1997. The presenilin 2 mutation (N141I) linked to familial Alzheimer disease (Volga German families) increases the secretion of amyloid β protein ending at the 42nd (or 43rd) residue. *Proc. Natl. Acad. Sci. USA*. 94:2025–2030.
Ucker, D.S., J. Myers, and P.S. Obermiller. 1992. Activation driven cell death: quantitative differences alone distinguish stimuli triggering nontransformed T cell proliferation or death. *J. Immunol.* 149:1583–1592.
Van Broeckhoven, C. 1995. Molecular genetics of Alzheimer's disease: identification of genes and gene mutations. *Eur. Neurol.* 35:8–19.
Vito, P., E. Lacana, and L.D. D'Adamio. 1996*a*. Interfering with apoptosis: Ca^{2+}-binding protein ALG-2 and Alzheimer's disease gene ALG-3. *Science (Wash. DC)*. 271:521–525.
Vito, P., B. Wolozin, J.K. Ganjei, K. Iwasaki, E. Lacana, and L.D. D'Adamio. 1996*b*. Requirement of the familial Alzheimer's disease gene PS2 for apoptosis. *J. Biol. Chem.* 271:31025–31028.
Yamatsuji, T., T. Matsui, T. Okamoto, K. Komatsuzaki, S. Takeda, H. Fukumoto, T. Iwatsubo, N. Suziki, A. Asami-Odaka, S. Ireland, et al. 1996. G protein-mediated neuronal DNA fragmentation induced by familial Alzheimer's disease-associated mutants of APP. *Science (Wash. DC)*. 272:1349–1352.
Walter, J., A. Capell, J. Grunberg, B. Presold, A. Schindzielorz, R. Prior, M.B. Podlisny, P. Fraser, P.H. St. George-Hyslop, D.J. Selkoe, and C. Hass. 1996. The Alzheimer's disease-associated presenilins are differentially phosphorylated proteins located predominantly within the endoplasmic reticulum. *Mol. Med.* 2:673–691.
Wasco, W., W.P. Pettingell, P.D. Jondro, S.D. Schmidt, S. Gurubhagavatula, L. Rodes, T. DiBlasi, D.M. Romano, S.Y. Guenette, D.M. Kovacs, et al. 1995. Familial Alzheimer's chromosome 14 mutations. *Nat. Med.* 1:848.
Wyllie, A.H. 1980. Cell death: significance of apoptosis. *Int. Rev. Cytol.* 68:251–306.
Wolozin, B., K. Iwasaki, P. Vito, J.K. Ganjei, E. Lacana, T. Sunderland, B. Zhao, J.W. Kusiak, W. Wasco, and L. D'Adamio. 1996. Participation of presenilin 2 in apoptosis: enhanced basal activity conferred by an Alzheimer mutation. *Science (Wash. DC)*. 274:1710–1713.
Wong, P.C., H. Zeng, H. Chen, M.W. Becher, D.J.S. Sirinathsinghji, M.E. Trumbauer, H.Y. Chen, D.L. Price, L.H.T. Van der Ploeg, and S.S. Sisodia. 1997. Presenilin 1 is required for Notch1 and Dll1 expression in the paraxial mesoderm. *Nature (Lond.)*. 387:288–292.
Xiao, J., and M.J. Monteiro. 1994. Identification and characterization of a novel (115 kDa) neurofilament-associated kinase. *J. Neurosci.* 14:1820–1833.